# Nonlinear dispersion in the Barrick-Weber equations

J.J. Green

23 March 2006

## 1 Introduction

An outstanding problem for the Barrick-Weber theory is its inaccuracy for waves of large wavenumber in high seas — the theory underestimates the observed backscatter for such waves. Consequently an inversion of the Barrick-Weber equations will overestimate the large-wavenumber component of high seas; this is particularly evident when the waves are propagating directly towards the radar.

In this note (not intended for publication in this form) we consider the effect of inclusion of the second-order correction to the dispersion relation on the predictions of the Barrick-Weber equations in seas where the wave-field is colinear with the incident radar.

## 2 Colinear waves

The Barrick-Weber theory predicts that the second-order component of the Doppler spectrum at radian Doppler frequency $\Omega$ is

$$\sigma_2(\Omega) = 2^7 \pi k_0^4 \sum_{m,m'=\pm 1} \iint_{\mathbb{R}^2} |\Gamma|^2 \, S(m\mathbf{k}) S(m'\mathbf{k}') \delta(\Omega - m w(\mathbf{k}) - m' w(\mathbf{k}')) \, \mathrm{d}\mathbf{p} \tag{1}$$

where $\mathbf{k} + \mathbf{k}_0 = \mathbf{p}$, $\mathbf{k}' + \mathbf{k}_0 = -\mathbf{p}$ and $\omega(\mathbf{k})$ is the temporal wave frequency at wavevector $\mathbf{k}$ (i. e., the dispersion relation).

In the case that the wave-field is colinear with the direction of the incident radar (either towards it or away from it) then (1) becomes a single integral of the wavenumber $k$

$$\begin{aligned} \sigma_2(\Omega) &= 2^7 \pi k_0^4 \sum_{m,m'=\pm 1} \int_{\mathbb{R}} |\Gamma|^2 \, S(mk) S(m'k') \delta(\Omega - m w(k) - m' w(k')) \, \mathrm{d}k \\ &= 2^7 \pi k_0^4 \sum_{m,m'=\pm 1} \int_{\mathbb{R}} |\Gamma|^2 \, S(mk) S(m'k') \delta(\Omega - \xi) \left| \frac{\mathrm{d}k}{\mathrm{d}\xi} \right| \mathrm{d}\xi \\ &= 2^7 \pi k_0^4 \sum_{m,m'=\pm 1} \sum_{\xi=\Omega} |\Gamma|^2 \, S(mk) S(m'k') \left| \frac{\mathrm{d}k}{\mathrm{d}\xi} \right| \end{aligned} \tag{2}$$

where we have introduced the variable $\xi = mw(k) + m'w(k')$ to solve the delta constraint. The result is that the integral is replaced in (2) by an explicit sum over all $k$ such that $\xi(k) = \Omega$.

The quantity $\Gamma$ is the *coupling coefficient*, consisting of hydrodynamic and electromagnetic contributions. We will neglect the latter and recall that, in the case that the (colinear) wave spectrum is wholly towards the radar, then $\Gamma = |k| + |k'|$.

# 3 Nonlinear dispersion

Barrick & Weber obtain the dispersion relation correct to second order as

$$\omega(\mathbf{k}) = \sqrt{g\,|\mathbf{k}|}(1 + \Delta_{\mathrm{pv}}(\mathbf{k}))$$

where $\Delta_{\mathrm{pv}}$ is the phase-velocity correction $\langle w_2/w_0 \rangle$, and obtain an expression for $\Delta_{\mathrm{pv}}$ in terms of the wavevector spectrum $S(\mathbf{k})$ (see below). In the colinear case we differentiate $\omega$ with respect to $k$ to obtain

$$\frac{\mathrm{d}\omega}{\mathrm{d}k} = \frac{1}{2}\,\mathrm{sgn}(k)\sqrt{\frac{g}{|k|}}(1 + \Delta_{\mathrm{pv}}(k)) + \sqrt{g\,|k|}\Delta'_{\mathrm{pv}}(k) = F(k),$$

say. Then since

$$\xi = m\omega(k) + m'\omega(k')$$

we have

$$\frac{\mathrm{d}\xi}{\mathrm{d}k} = mF(k) - m'F(k)$$

and so find the Jacobian of (2).

# 4 Ideal Philips wave-spectrum

As a specific example of a unidirectional wave-spectrum we take

$$S(k) = \begin{cases} 0 & (k < k_{\mathrm{p}}) \\ B/2k^3 & (k > k_{\mathrm{p}}) \end{cases}$$

which is an ideal Philips spectrum. Here $B$ is a constant determined experimentally to have the value 0.05 and $k_{\mathrm{p}}$, the wavenumber of the spectral peak, is conveniently written in terms of the significant waveheight, $h$. By Longuet-Higgins

$$h^2 = 16 \int S(k)\,\mathrm{d}k = 4B/k_{\mathrm{p}}^2$$

so that $k_{\mathrm{p}} = 2\sqrt{B}/h$. With this spectrum Barrick & Weber find that the phase-velocity correction can be found explicitly as

$$\begin{aligned} \Delta_{\mathrm{pv}}(k) &= \frac{2k}{\sqrt{g\,|k|}} \int_0^\infty \sqrt{g\,|p|}\,\min\{k, p\} S(p)\,\mathrm{d}p \\ &= \frac{2B}{3} \begin{cases} 3(k/k_{\mathrm{p}})^{1/2} - 2 & (0 < k_{\mathrm{p}} < k) \\ (k/k_{\mathrm{p}})^{3/2} & (0 < k < k_{\mathrm{p}}) \end{cases} \end{aligned} \tag{3}$$

for $k > 0$, and defined by oddness for $k < 0$.

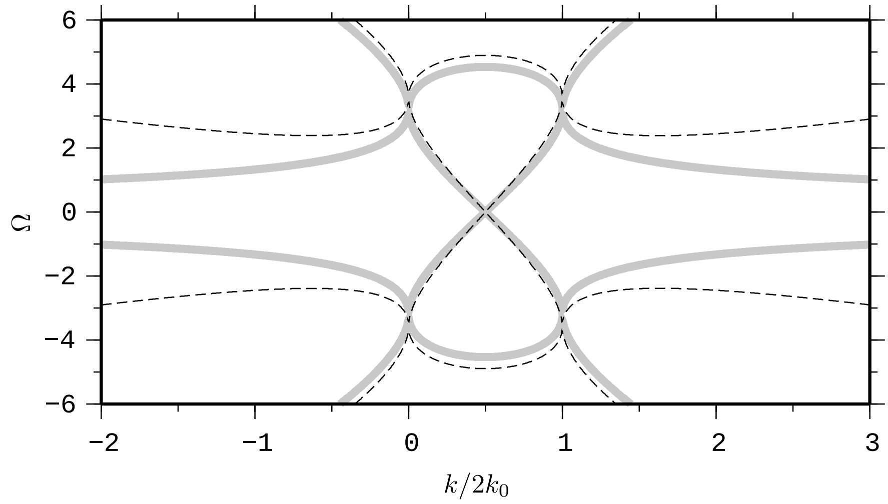


Figure 1: Solutions to $\Omega = m\omega(k) + m'\omega(k')$ for linear (grey) and non-linear (dashed) dispersion relations

# 5 Consequences

We can now find how replacing the linear dispersion relation with the nonlinear affects the theoretical Doppler spectrum for an ideal unidirectional Philips wave-spectrum (3). In (2) we sum over $k$ such that

$$\begin{aligned} \Omega &= m\sqrt{g\,|k|}(1+\Delta_{\mathrm{pv}}(k)) + m'\sqrt{g\,|k'|}(1+\Delta_{\mathrm{pv}}(k')) \\ &= \Omega_{\mathrm{B}} + m\sqrt{g\,|k|}\Delta_{\mathrm{pv}}(k) + m'\sqrt{g\,|k'|}\Delta_{\mathrm{pv}}(k') \end{aligned}$$

where $\Omega_{\mathrm{B}}$ is the linear part. For a unidirectional wave-field we must have $mk$ and $m'k'$ positive in order for the contribution in (2) to be nonzero. From this, and the oddness of $\Delta_{\mathrm{pv}}$, we see that all of the relevant solution branches must be shifted upwards when compared to using just $\Omega_{\mathrm{B}}$ in (4). This is illustrated in Figure 1, where (as in the rest of this report) we have taken a radar frequency of 25MHz and significant waveheight of 5m.

The shifting of the solution manifold is most pronounced for the branches for which $mm' = -1$, the outer branches. In the linear case (grey) the branches tend to zero for large $k$, but these diverge when the nonlinear effects are included (shown dashed).

Consider the right-hand lower branch in the positive quadrant in Figure 1, corresponding to $m = 1$, $m' = -1$. In the linear case we have

$$\Omega_{\mathrm{B}} = \sqrt{g\,|k|} - \sqrt{g\,|k'|}$$

and since $k + k' = 2k_0$, $k > 0$ and $k' < 0$ on this branch we clearly have $k = 2k_0 - k' > 2k_0$ so

$$|k'|^{1/2} = k^{1/2}(1 - 2k_0/k)^{1/2}$$

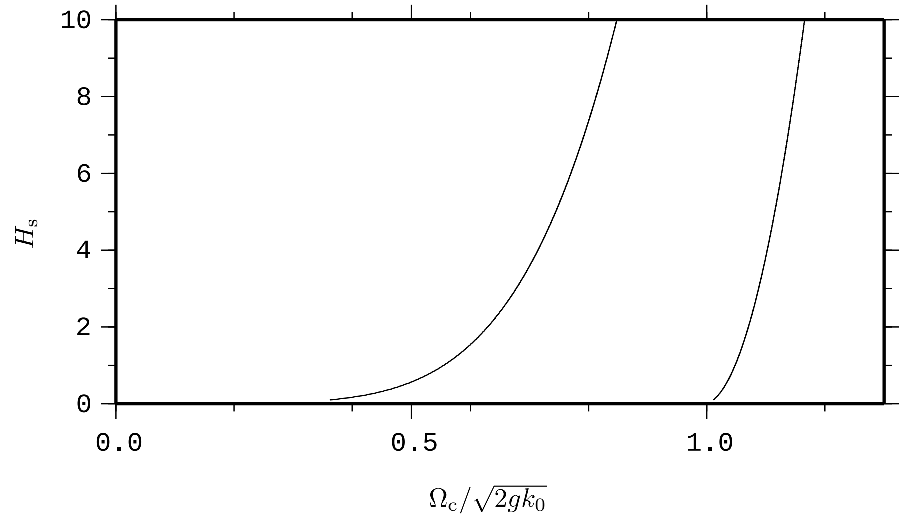


Figure 2: The values of $\Omega_c$ (left) and the location of the corrected first-order peak (right), relative to $\sqrt{2gk_0}$, for various significant waveheights

and we can expand the term in parentheses with the binomial theorem:

$$\left(1 - \frac{2k_0}{k}\right)^{1/2} = 1 - \frac{k_0}{k} - \left(\frac{k_0}{2k}\right)^2 - \cdots$$

and so

$$\begin{aligned}\Omega_B &= \sqrt{g\,|k|} - \sqrt{g\,|k|}(1 - k_0/k - (k_0/2k)^2 - \cdots) \\ &= k_0\sqrt{g/k}(1 + k_0/2k + \cdots) \to 0\end{aligned}$$

as $k \to \infty$. However, the nonlinear corrections is

$$\begin{aligned}\sqrt{g\,|k|}\Delta_{pv}(k) - \sqrt{g\,|k'|}\Delta_{pv}(k') &= \sqrt{g}(|k|^{1/2}\,\Delta_{pv}(k) + |k'|^{1/2}\,\Delta_{pv}(-k')) \\ &\approx 2\sqrt{g\,|k|}\Delta_{pv}(k)\end{aligned}$$

which is $O(k)$ for large $k$, since $\Delta_{pv}(k) = O(\sqrt{k})$.

The change in behaviour for the outer (i.e., $mm' = -1$) branches has consequences for the number of solutions to the inner sum in (2): in the linear case we always have $k$ such that $\Omega = \Omega_B(k)$, but when the nonlinear correction is included we find that there are no solutions for $|\Omega|$ less that some critical value $\Omega_c$ and exactly two solutions for $|\Omega| > \Omega_c$. If we assume that $k_p < k_0$ (which will be the case in realistic seas) we find that $\Omega_c$ is the root of a quintic in $\sqrt{k}$, so we solve for it numerically as shown in Figure 2.

The primary effect of inclusion of the nonlinear term into the delta constraint in (2) is a shift of the whole Doppler spectrum by a frequency $\sqrt{2gk_0}\Delta_{pv}(2k_0)$, accounting for the Stokes-drift component of the current. In Figure 3 this current effect is removed to aid comparison between linear and nonlinear. We can see a singularity at the minimal Doppler frequency, $\Omega_c$, and an apparent reversal and stretching of the innermost part of the linear spectrum, outward

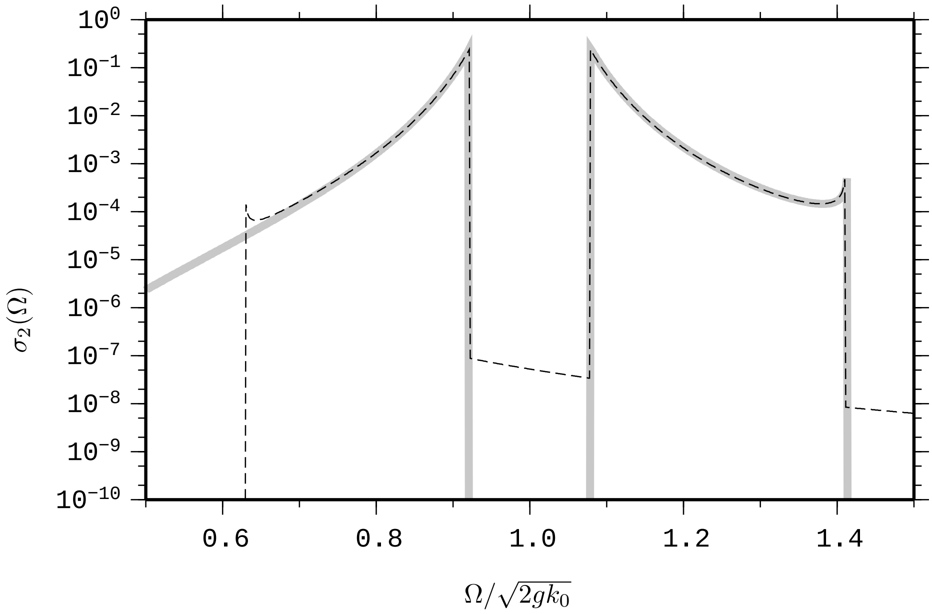


Figure 3: The predicted Doppler spectrum $\sigma_2(\Omega)$ with linear (grey) and nonlinear (dashed) dispersion relation.

towards large $\Omega$. But these effects seem to be the only visible differences between the linear and nonlinear cases.

Note that the delta constraint in (2) is not the only place in which the dispersion relations occurs, but we find that the coupling coefficient

$$\Gamma = \Gamma(k, w(k), k', w(k'))$$

is unaffected in the colinear wave case, and that Jacobian $1/\,|mF(k) - m'F(k)|$ is only minimally modified in the unidirectional case. As can be seen in the comparisons in Figure 4, the nonlinear Jacobian is within a few percent of the linear for all but the outer branches in the $mm' = 1$ case; on these branches one of $k$ or $k'$ is negative and so $S(mk)S(m'k)$ must be zero in the unidirectional case.

# 6 Conclusions

In the unidirectional wave-field case, the effect of inclusion of the nonlinear term in the dispersion relation in the Barrick-Weber theory is restricted to a shift in the Doppler spectrum, accounting for the Stokes drift, and the emergence of a minimal Doppler frequency $\Omega_{\mathrm{c}}$ below which the spectrum vanishes. The only observable consequence might be the singularity at $\Omega_{\mathrm{c}}$, which does contain some information on the ocean state (albeit rather weak information).

It is clear that the overestimation of the decay of $\sigma(\Omega)$ away from the first order peaks is *not* being corrected by inclusion of nonlinear dispersion; at least for a unidirectional model. This situation *might* change for a bidirectional wave-field, for then we would find nonzero contributions to (2) for $k$ and $k'$ where the

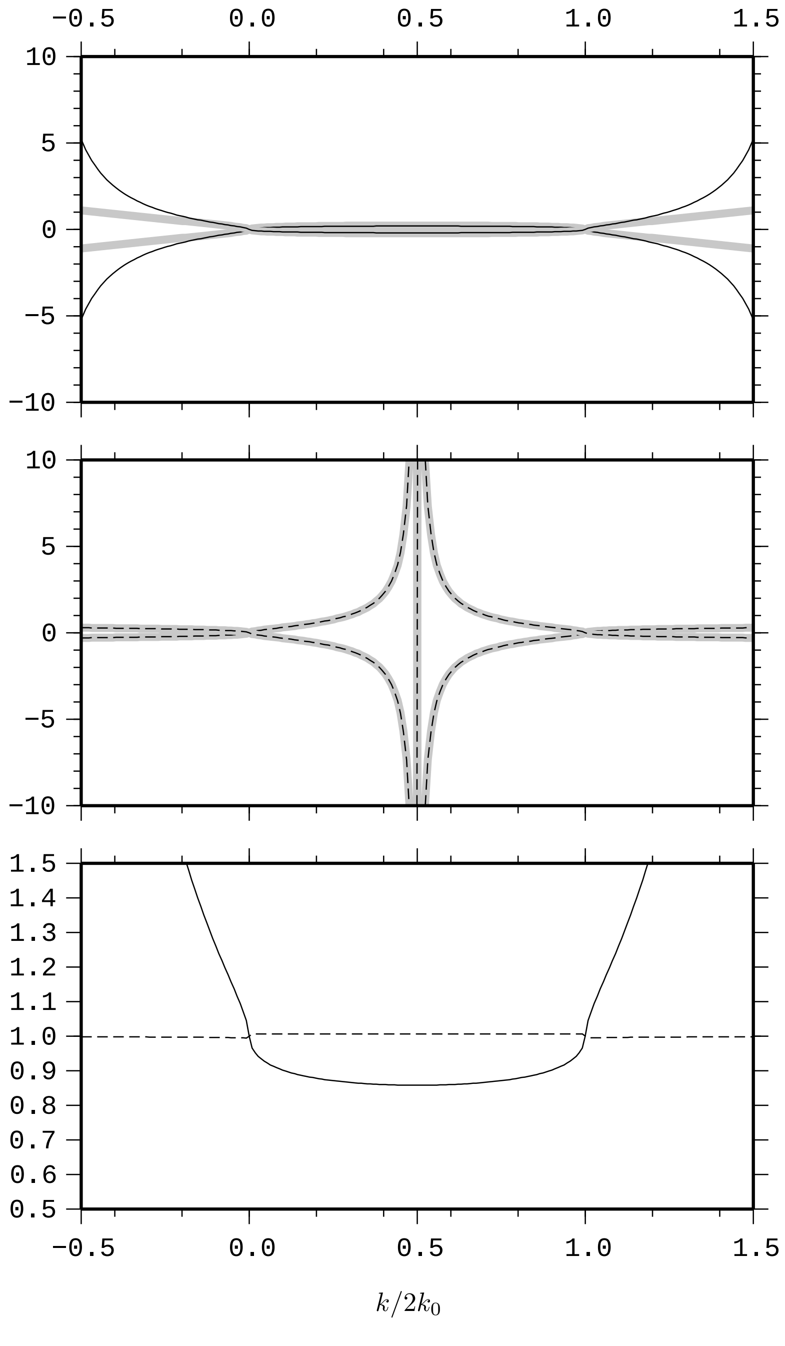


Figure 4: Values of $1/(mF(k)-m'F(k'))$ with linear (grey) and nonlinear (solid, dashed) dispersion relations. Upper frame, $mm' = 1$; middle frame, $mm' = -1$; bottom frame, the ratio of linear and nonlinear Jacobian for $mm' = 1$ (solid) and $mm' = -1$ (dashed).

Jacobian is enhanced in the nonlinear $mm' = 1$ case, as shown in the bottom frame of Figure 4.

To obtain a sense of the effect of two-dimensionality in these calculations we have plotted the integration contours using the two-dimensional version of the Barrick-Weber equations, linear and corrected, as shown in Figure 5. The effects are noticable in the $mm' = 1$ case (left column) but barely discernable in the $mm' = -1$ case (right).

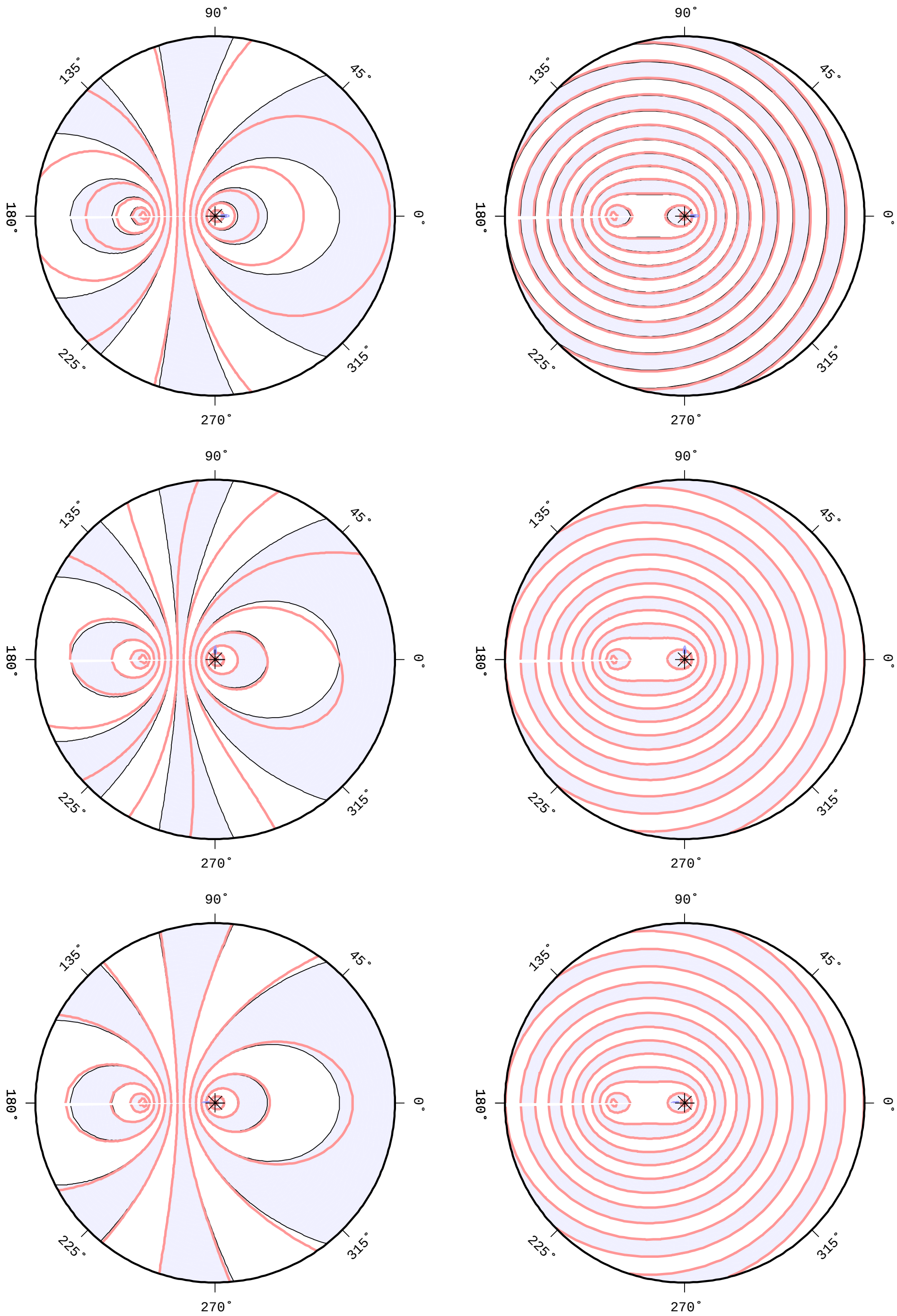


Figure 5: Barrick-Weber integration contours in the two-dimensional case: for Philips spectrum in the directions 0° (waves towards radar), 90° and 180°; contours are shown black in the linear case and red in the corrected case.